SUPPLEMENTARY INFORMATION

Sensitive radio-frequency measurements of a quantum dot by tuning to perfect impedance matching

N. Ares,[1] F.J. Schupp,[1] A. Mavalankar,[1] G. Rogers,[1] J. Griffiths,[2] G.A.C. Jones,[2] I. Farrer,[2] D.A. Ritchie,[2] C.G. Smith,[2] A. Cottet,[3] G.A.D. Briggs,[1] and E.A. Laird[1]

[1] *Department of Materials, University of Oxford, Parks Road, Oxford OX1 3PH, United Kingdom*
[2] *Cavendish Laboratory, J. J. Thomson Avenue, Cambridge CB3 0HE, United Kingdom*
[3] *Laboratoire Pierre Aigrain, Ecole Normale Supérieure-PSL Research University, CNRS, Université Pierre et Marie Curie-Sorbonne Universités, Université Paris Diderot-Sorbonne Paris Cité, 24 rue Lhomond, 75231 Paris Cedex 05, France*

(Dated: March 7, 2016)

I. CIRCUIT SIMULATION OF THE MATCHING NETWORK

The fits in Fig. 2 are obtained using the circuit model shown in Fig. S1. The three capacitors C_S, C_D and C_M are taken as simple lumped elements, each incorporating any parasitic capacitance in parallel with the varactor. The inductor is modelled as a network of elements as shown, which simulate its self-resonances and losses. Other losses in the circuit are modelled by an effective resistance R. The device under test is taken as a parallel RC circuit.

The reflection coefficient Γ is then equal to

$$\Gamma(f_\mathrm{C}) = \frac{Z_\mathrm{tot}(f_\mathrm{C}) - Z_0}{Z_\mathrm{tot}(f_\mathrm{C}) + Z_0}, \tag{S1}$$

where Z_tot is the total impedance from the circuit's input port and $Z_0 = 50\ \Omega$ is the line impedance. We relate the measured transmission S_{21} to Γ by assuming a constant overall insertion loss A, incorporating attenuation in the cryostat lines, the coupling of the directional coupler, and the gain of the amplifier, such that

$$|S_{21}(f_\mathrm{C})| = A|\Gamma(f_\mathrm{C})|. \tag{S2}$$

Fitting to Eq. (S2), we take $C_\mathrm{D} = 87$ pF from the known component value; take $L = 223$ nH, $R_\mathrm{L} = 3.15 \times 10^{-4}\ \Omega \times \sqrt{f_\mathrm{C}\ [\mathrm{Hz}]}$, $\mathrm{R_C} = 25\ \Omega$ and $\mathrm{C_L} = 0.082$ pF from the datasheet of the inductor; and assume $R_\mathrm{dot} = 1$ GΩ and $C_\mathrm{dot} = 1$ aF for a pinched-off device. Fit parameters are then A, C_M, R, and C_S. From the fit at $V_\mathrm{S} = 13.5$ V, we obtain $A = -27.6 \pm 0.3$ dB and $C_\mathrm{M} = 14.5 \pm 0.9$ pF. For other fits, we hold these values constant; extracted values for C_S and R at each voltage are plotted in Fig. S2.

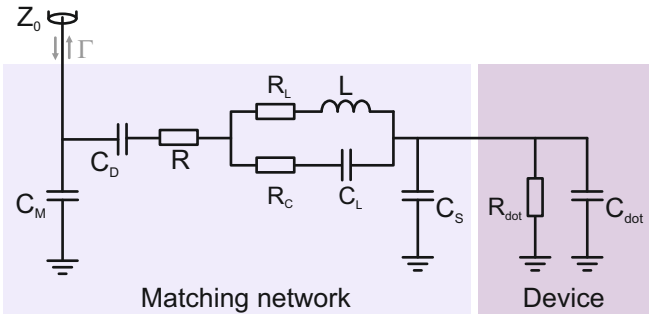

FIG. S1. Circuit model of the matching network and device. Capacitors C_M, C_D and C_S are taken as simple lumped elements, including any parasitic capacitances in parallel. Elements R_L, R_C and C_L model parasitic contributions to the impedance of the inductor L. The effective resistance R models other losses in the circuit. The quantum dot is modelled by the combination of $R_\mathrm{dot} = 1/G_\mathrm{dot}^\mathrm{RF}$ and C_dot.

II. CIRCUIT SENSITIVITY

In this section we give further details of how the sensitivities in Fig. 3 are measured and simulated.

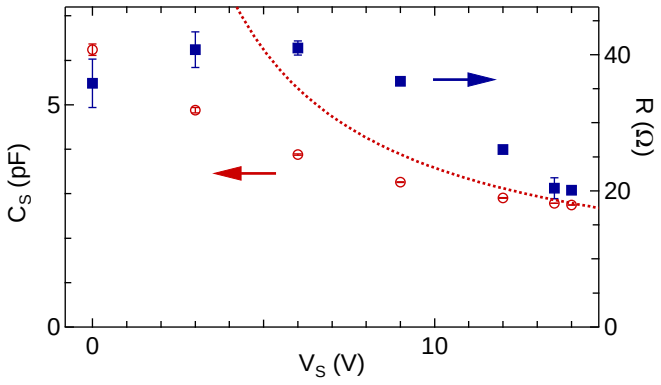

FIG. S2. Values of C_S and R at $T_\mathrm{MC} = 1$ K, obtained from fits as in Fig. 2(a). Dashed line is the datasheet value of C_S at room temperature including a parasitic capacitance of 0.7 pF. The comparatively small fitted values of C_S indicate that some of the dopants in the varactor have frozen out.

A. Measuring the sensitivity

For the sensitivity measurement in Fig. 3, we determine the root-mean-square (RMS) capacitance modulation δC_S as follows. From a measurement of $|S_{21}|$ as a function of f_C and V_S (Fig. S3(a)), we extract the resonance frequency $f_0(V_S)$, defined as the location of the minimum at each voltage. Approximating that

$$f_0(V_S) \approx \frac{1}{2\pi\sqrt{LC_S(V_S)}}, \tag{S3}$$

we relate δC_S to the RMS varactor modulation voltage V_m by:

$$\begin{aligned}\delta C_S &= \left|\frac{dC_S}{dV_S}\right| V_m \\ &= \frac{V_m}{2\pi^2 L f_0^3}\left|\frac{df_0}{dV_S}\right|,\end{aligned} \tag{S4}$$

where df_0/dV_S is taken as a smoothed numerical derivative of the measured $f_0(V_S)$ (Fig. S3(b)).

Although Eq. (S3) applies strictly only for a simple LC resonator, we have confirmed numerically that this procedure gives a good approximation for dC_S/df_0 in our circuit model.

B. Simulating the sensitivity

Taking the amplitude of the incident signal as V_{in}^0, the reflected signal from the matching network is:

$$V_r(t) = V_{in}^0\ \mathrm{Re}(\Gamma e^{i\omega t}).$$

In response to a change δC_S in the capacitance, the reflection coefficient changes by $\delta\Gamma$, leading to a change in reflected voltage:

$$\delta V_r(t) = V_{in}^0\ \mathrm{Re}(|\delta\Gamma| e^{i(\omega t + \arg(\delta\Gamma))}),$$

giving for the variance in V_r

$$\begin{aligned}\langle \delta V_r^2\rangle &= \frac{(V_{in}^0)^2}{2}\langle|\delta\Gamma|^2\rangle \\ &= \frac{(V_{in}^0)^2}{2}\left|\frac{d\Gamma}{dC_S}\right|^2 \langle \delta C_S^2\rangle.\end{aligned}$$

The sensitivity is defined as the root-mean-square δC_S per unit bandwidth for which $\langle \delta V_r^2\rangle$ becomes equal to the noise fluctuation $S_V^2 \Delta f$:

$$S_C = \frac{\sqrt{2}}{\left|\frac{d\Gamma}{dC_S}\right| V_{in}^0} S_V.$$

Assuming that the system noise is dominated by the amplifier noise temperature T_N and that there are no losses between the matching circuit and the amplifier input, we obtain:

$$S_C = \frac{\sqrt{2kT_N Z_0}}{\left|\frac{d\Gamma}{dC_S}\right| V_{in}^0}, \tag{S5}$$

where k is Boltzmann's constant. This is the formula used to simulate S_C in Fig. 3.

In this simulation, we took the amplifier noise from the manufacturer's specification, giving $T_N = 3.7$ K. We calculated $\left|\frac{d\Gamma}{dC_S}\right|$ numerically using the same circuit model as above, taking parameters from fits as in Fig. 2. The signal level to the matching circuit, V_{in}^0, is in principle known from the applied power $P_1 = -29$ dBm and the insertion loss in the injection line. However, we find that the fits in Fig. 2 yield an overall insertion loss ($A = -27.6 \pm 0.3$ dB) that is greater than the sum of the fixed attenuators on the injection line (-31 dB), the coupling of the directional coupler (-20 dB), and the specified amplifier gain (+32 dB). This implies a distributed additional insertion loss of ~ -8.6 dB, with a corresponding uncertainty in the value of V_{in}^0. For the simulations in Fig. 3, we assumed this contribution was distributed equally before and after the matching network, but the possibility of unequal distribution dominates the error bars in simulated S_C and $S_C V_0$.

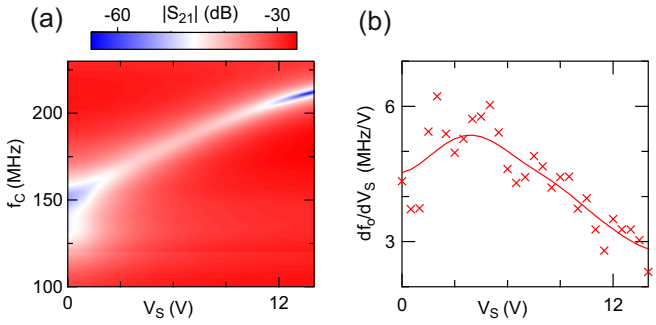

FIG. S3. (a) Response of the circuit as a function of V_S and f_C. (b) Points: Numerical derivative (df_0/dV_S) as a function of V_S. Line: Smoothed data used in Eq. (S4) to calculate δC_S.

C. The figure of merit for readout bandwidth

In the main paper, we stated that the figure of merit for a dispersive qubit readout circuit is not the capacitance sensitivity S_C, but rather the product $S_C V_0$. In this section, we justify this statement. For any transition being measured, such as the inter-dot transition in a double-dot qubit, the quantum capacitance peaks in a window about zero detuning. Although Eq. (S5) predicts an improving capacitance sensitivity with increasing incident signal, once the detuning excitation becomes larger than the peak width, over most of the detuning cycle

the device is configured to have zero capacitance. The benefit of the larger drive voltage is therefore lost.

To calculate the bandwidth with which the inter-dot transition can be resolved, we note that the average capacitance over the RF cycle is

$$\overline{C} = \frac{\Delta q}{\Delta V}$$

where $\Delta V = 2\sqrt{2}V_0$ is the peak-to-peak voltage on the source electrode and Δq is the change in electrode charge over the cycle. The maximum value of Δq is achieved when V_0 is set much larger than the peak width, and is given by $\Delta q = \lambda e$, where λ is the lever arm. The readout bandwidth Δf for unit SNR then satisfies:

$$\sqrt{\Delta f} = \frac{\overline{C}}{S_C} = \frac{\Delta q}{2\sqrt{2}S_C V_0} = \frac{\lambda e}{2\sqrt{2}S_C V_0}. \quad \text{(S6)}$$

For given lever arm, the figure of merit is therefore given by $S_C V_0$, which from Eq. (S5) is fixed by the circuit parameters independent of the incident power. For the optimum tuning of this circuit, we have $S_C V_0 = 1.2 \times 10^{-3} e/\sqrt{\text{Hz}}$, so for $\lambda = 0.3$ we could achieve unit SNR for single-shot readout in bandwidth $\Delta f = 7.8$ kHz, or an integration time of 64 μs.

III. CARRIER SIGNAL POWER

The carrier power in Fig. 4(a) was chosen separately at each frequency f_C to avoid broadening the Coulomb peak. Fig. S4(a) shows this peak broadening for increasing P_1 for a typical combination of f_C and V_S. For each such combination, a threshold power P_T is extracted, defined as the largest power for which no peak broadening could be detected. Figure S4(b) shows how this threshold power depends on f_C for two different V_S settings. Each dataset is fitted to a Lorentzian to define a function $P_T(f_C, V_S)$. This is the carrier power chosen in Fig. 4(a).

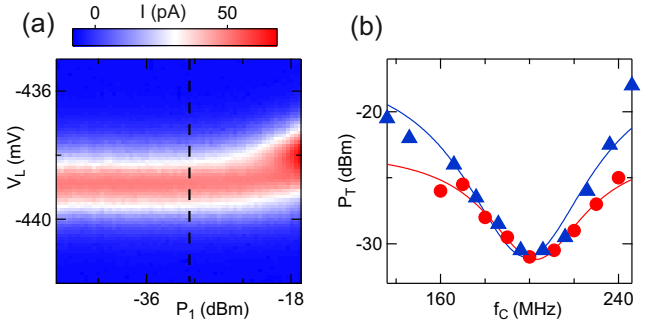

FIG. S4. (a) Current as a function of V_L and P_1, showing the Coulomb peak at which the SNR measurements in Fig. 4(a) and (b) were performed. For these data, $V_S = 13.5$ V, $f_C = 211$ MHz, and $V_{bias} = 100$ μV. The dashed line indicates the threshold carrier power P_T; for $P_1 < P_T$ no detectable broadening of the Coulomb peak is observed. (b) Measured P_T (points) as a function of carrier frequency for $V_S = 9$ V (triangles) and $V_S = 13.5$ V (circles). Solid lines are Lorentzian fits from which values of P_1 were chosen for the SNR measurements in Fig. 4(a).

IV. MEASUREMENT OF THE QUANTUM DOT CAPACITANCE

To determine the device capacitance C_{dot} as in Fig. 5(b), we begin by measuring $|S_{21}(f_C)|$ with V_L set so that the device is pinched off. In this situation, we assume that $C_{dot} = 0$. Fitting as in Fig. 2, we obtain $C_S = 2.673 \pm 0.005$ pF, $C_M = 15.0 \pm 0.8$ pF, $R = 11.7 \pm 0.9$ Ω and $A = -24.9 \pm 0.2$ dB. The differences from the values at 1 K indicate that parasitic losses are reduced at 20 mK.

Given these circuit parameters, the phase of the reflected signal for other V_L settings is determined entirely by C_{dot} and R_{dot}; from Eq. (S1), Γ can be expressed in terms of an amplitude (A_v) and a phase (ϕ) as follows,

$$\Gamma = A_v(Z_{tot})e^{i\phi(Z_{tot})}, \quad \text{(S7)}$$

where $Z_{tot} = Z_{tot}(R_{dot}, C_{dot})$. Eq. (S7) makes explicit how the phase shift measured as in Fig. 5(a) is dependent on both R_{dot} and C_{dot}, as mentioned in the paper. While the phase shift extracted from the curves in Fig. 5(a) corresponds directly to ϕ, the conversion from the amplitude of the demodulated signal (V_D) to A_v is not equally straightforward; it depends on the overall circuit gain that we cannot determine accurately due to small non-linearities. For this reason, as mentioned in the paper, we have just relied on the measured phase shift to determine C_{dot}.

Finally, from the measured phase shift as a function of V_L, obtained by fitting curves similar to Fig. 5(a), and assuming $R_{dot} = 1/G^{DC}_{dot}$, we numerically evaluate C_{dot} to obtain the values plotted in Fig. 5(b).

V. PROPORTIONALITY BETWEEN QUANTUM DOT CAPACITANCE AND CONDUCTANCE

This section presents a simple model which explains the relationship between G^{DC}_{dot}, G^{RF}_{dot} and C_{dot}. We consider a quantum dot coupled to left and right leads by tunnel rates Γ_L and Γ_R respectively, and assume the low-temperature limit $kT_{MC}/\hbar \ll \Gamma_R, \Gamma_L$. The linear DC conductance can then be written

$$G^{DC}_{dot} = \frac{2e^2}{h}\frac{\Gamma_L\Gamma_R}{\Gamma_L + \Gamma_R}\rho(\epsilon_F, V_L) \quad \text{(S8)}$$

where ρ is the quantum dot density of states, ϵ_F is the the Fermi level and V_L the gate voltage that allows us

to control the electrochemical potential of the quantum dot [1].

We now consider a time-dependent voltage $V(t) = \sqrt{2}V_0 \cos\omega t$ applied to the left lead. The current that flows in response to this voltage is not in general [2, 3] determined by Eq. (S8). However, so long as $\omega \ll \Gamma_\mathrm{L}, \Gamma_\mathrm{R}$, electron tunnelling occurs instantaneously on the timescale of the oscillating voltage and there is no additional dissipation due to the time dependence. From the width of the smallest Coulomb peak in Fig. 5(b), we deduce $\Gamma_\mathrm{L} + \Gamma_\mathrm{R} \sim 30$ GHz, and therefore this assumption is justified. The RF conductance is therefore the same as the DC conductance:

$$G^\mathrm{RF}_\mathrm{dot} = G^\mathrm{DC}_\mathrm{dot}.$$

A capacitance arises because the quantum dot charges and discharges in response to the RF voltage. The charge on the dot is

$$Q(t) = Q_0 + e\kappa\rho(\epsilon_\mathrm{F}, V_\mathrm{L})V(t)$$

where Q_0 is the charge with no bias, e is the elementary charge, and κ is the occupation probability of a state in the transport window. To supply this charge, the current from the left lead is

$$\begin{aligned} I(t) &= \beta\dot{Q}(t) \\ &= e\beta\kappa\rho(\epsilon_\mathrm{F}, V_\mathrm{L})\dot{V}(t) \end{aligned}$$

with β a constant which parameterizes how much of the charge tunnels from the left lead, as well as how plasmonic screening currents triggered by tunneling events are distributed in the circuit [4]. We identify this current as due to a capacitance

$$C_\mathrm{dot} = e\beta\kappa\rho(\epsilon_\mathrm{F}, V_\mathrm{L}).$$

Comparing with Eq. (S8), we see that

$$C_\mathrm{dot} = \beta\kappa\frac{\Gamma_\mathrm{L} + \Gamma_\mathrm{R}}{\Gamma_\mathrm{L}\Gamma_\mathrm{R}} G^\mathrm{DC}_\mathrm{dot}.$$

In the general case, C_dot and $G^\mathrm{DC}_\mathrm{dot}$ should not be exactly proportional since β, κ, and the tunnel rates vary independently with V_L. We cannot determine the full dependence of $\beta\kappa$ with the tunnel rates Γ_L and Γ_R from our phenomenological model. However, in the limit where $\Gamma_\mathrm{R} \ll \Gamma_\mathrm{L}$ and only Γ_L increases with V_L, $\beta\kappa$ should saturate to its asymmetric limit, while $\frac{\Gamma_\mathrm{L}+\Gamma_\mathrm{R}}{\Gamma_\mathrm{L}\Gamma_\mathrm{R}} \simeq \frac{1}{\Gamma_\mathrm{R}}$ should remain constant. In this case, the variations of C_dot and $G^\mathrm{DC}_\mathrm{dot}$ with V_L should be proportional. From our conductance data, we can see that Γ_R and Γ_L are clearly asymmetric. Therefore this scenario could explain why we find that C_dot and $G^\mathrm{DC}_\mathrm{dot}$ are proportional.

[1] Y. Meir, N.S. Wingreen, and P.A. Lee, "Transport through a strongly interacting electron system: Theory of periodic conductance oscillations." Phys. Rev. Lett. **66**, 3048–3051 (1991).

[2] J. Gabelli, G. Fève, J.-M. Berroir, B. Plaçais, A. Cavanna, B. Etienne, Y. Jin, and D. C. Glattli, "Violation of kirchhoff's laws for a coherent rc circuit." Science (New York, N.Y.) **313**, 499–502 (2006).

[3] S. J. Chorley, J. Wabnig, Z. V. Penfold-Fitch, K. D. Petersson, J. Frake, C. G. Smith, and M. R. Buitelaar, "Measuring the complex admittance of a carbon nanotube double quantum dot." Phys. Rev. Lett. **108**, 036802 (2012).

[4] Ya.M. Blanter and M. Büttiker, "Shot noise in mesoscopic conductors," Phys. Rep. **336**, 1–166 (2000).